Frontiers in Engineering
ISSN Print: 3104-4298
ISSN Online: 3104-4301
CD ISSN: 3104-431X
https://doi.org/10.63313/FE.2001

Hydrodynamic Lubrication Mechanism and CFD Analysis of Tesla-Valve Microtextures

Jing Li. Fazhan Yang
Qingdao University of Technology, Qingdao 266520, China

How to cite this paper: Li, J., & Yang, F. Z. (2025). Hydrodynamic Lubrication Mechanism and CFD Analysis of Tesla-Valve Microtextures. Frontiers in Engineering, 1(1), 1-8. ISSN Print: 3104-4298, ISSN Online: 3104-4301.
https://doi.org/10.63313/FE.2001
Published: 2025-09-25

Abstract

Titanium alloys are widely used in aerospace and medical industries owing to their high strength, low thermal conductivity and excellent corrosion resistance. However, their high chemical reactivity and poor heat dissipation cause severe tool wear during cutting. Surface microtexturing has been proven to significantly improve the lubrication performance of friction pairs and extend service life. To explore the lubrication mechanism of Tesla-valve microtextures, femtosecond laser machining was employed to fabricate micrometer-scale Tesla-valve structures on YG8N cemented carbide surfaces. A three-dimensional model was established in Fluent, and the velocity and pressure distributions at various inlet flow rates were simulated. The results show that at low speeds ($v \leqslant 2$ m/s), the microtexture exhibits higher reverse than forward flow velocity, with superior reverse hydrodynamic lubrication performance; whereas at high speeds ($v \geqslant 3$ m/s), the forward flow velocity exceeds the reverse, leading to improved forward hydrodynamic lubrication performance. As flow rate increases, the vortex region and pressure potential inside the microtexture expand significantly, enhancing the load-carrying capacity of the oil film.

Keywords

Tesla valve microtexture; fluid simulation; femtosecond laser machining; frictional direction; friction and wear

Introduction

The surface friction characteristics of mechanical transmission and contact components directly affect the operating efficiency and reliability of the entire system [1]. The progressive accumulation of frictional resistance between mating pairs accelerates wear and energy loss, thereby shortening service life. With the rapid development of modern industry, research on the lubrication, wear resistance, and drag-reduction properties of frictional interfaces has become increasingly intensive. Hamilton et al. [2]first demonstrated that introducing micro-textures onto friction surfaces can generate a hydrodynamic lubrication effect, thereby improving interfa-

cial lubrication and extending the service life of mechanical components.

Continuous optimization of microtexture geometries has led to the proposal of Tesla-valve-type microtextures and their application in fluid-lubricated systems[3]. Liu et al.[4] found that, under identical flow rates, reverse flow at the abrupt bends of a Tesla valve is more prone to vortex formation due to the reduced cross-sectional area, resulting in local pressure losses compared with forward flow. Huang et al. [5] analyzed the lateral and longitudinal vortices generated when fluid enters a Tesla-valve channel at different angles and reported that lateral vortices help equalize the velocity distribution and accelerate the flow. Using fluid simulations, Duo et al. [6]showed that gears incorporating Tesla-valve textures exhibit roughly four times the lubrication performance of untextured gears, while also improving surface wear resistance and reducing wear volume by about 66.7%, thereby effectively enhancing lubrication and friction behavior and extending gear life.

Current studies of Tesla valves are largely limited to simulating their macroscopic lubrication performance, with relatively little work addressing lubrication mechanisms at the micro- and nanoscale. In this study, computational fluid dynamics (CFD) was employed to analyze the effect of Tesla-valve microtextures on the friction and lubrication behavior of material surfaces, and the flow-lubrication characteristics were further validated through friction and wear experiments.

1. Fluent Fluid Simulation

The Tesla valve exhibits a distinctive diode-like characteristic. When fluid flows forward through the Tesla-valve microtexture, most of it bypasses the curved channel and continues along the main passage with low resistance. In contrast, during reverse flow, a blocking effect occurs at the intersection between the straight and curved channels. After diversion, a larger portion of the fluid enters the curved channel and collides with the flow in the main passage, resulting in increased resistance. Owing to this unique one-way conduction property, the Tesla valve offers significant advantages in microfluidic applications.

A Tesla-valve microtexture model was built in SolidWorks with an inlet dimension of 1.5 mm × 2 mm, identical to the outlet. The model was then imported into the ANSYS finite-element software, and meshed using the Fluent Mesh module with a grid size of 0.1 mm. The left boundary was defined as a velocity inlet, the right as a pressure outlet, and all other surfaces as walls. Because the path of the lubricant varies depending on its direction of entry, the flow from the bifurcation merging into the main channel was defined as the forward direction, and the opposite direction as reverse.

The three-dimensional Tesla-valve model was simulated using Fluent. To simplify the problem, the following assumptions based on fluid mechanics were made for the lubricant in the microtexture:

(1) The lubricant is treated as an incompressible Newtonian fluid [7];

(2) Its physical properties are independent of temperature [8];

(3) Density and viscosity are constant throughout the 3D model domain;
(4) Thermal radiation effects are neglected.

Under normal conditions, the lubricant flows in an orderly manner with a uniform velocity. However, when passing through the Tesla-valve microtexture channel, its flow velocity changes markedly, and turbulence, convection, and strong vortex phenomena occur at the channel intersections [9]. The simulation employed the k–ε turbulence model. Boundary conditions were set as an inlet and outlet pressure of 101 kPa, with different inlet velocities of 0.5 m/s, 1 m/s, 3 m/s, 6 m/s, and 9 m/s. Pressure–velocity coupling was achieved using the SIMPLE algorithm, and the second-order upwind scheme was applied for discretizing the energy and momentum equations. The lubricant density was set at 840 kg/m^3 and its dynamic viscosity at 0.041 Pa·s. The maximum iteration count was 2000, with a convergence criterion of not less than 10^{-5}. Because the cross-sectional area inside the Tesla-valve microtexture remained constant, the lubricant film thickness was assumed constant as well, with h=1.5 mm. The load-carrying capacity F_s of the lubricant film surface was obtained by integrating the pressure p over the entire film area, while the friction force F_f was determined by integrating the shear stress τ generated in the lubricant film:

$$F_s = \iint p\, ds \tag{1}$$

$$F_f = \iint \tau\, ds \tag{2}$$

where s is the contact area of the textured surface (m^2).

The coefficient of friction is calculated as the ratio of the oil-film load-carrying capacity to the friction force according to Eqs. (2) and (3):

$$f = \frac{F_f}{F_s} \tag{3}$$

2. Results and Discussion

Table 1 presents the variations in velocity and pressure of the Tesla-valve microtexture at different lubricant flow rates. It is observed that when the initial flow velocity of the lubricant is below 2 m/s, the reverse flow velocity exceeds the forward flow velocity. Conversely, when the flow velocity is greater than 3 m/s, the forward flow velocity is higher than the reverse, and the velocity difference between the two directions increases with increasing inlet velocity. At flow velocities below 2 m/s, the forward pressure is higher than the reverse pressure, whereas at flow velocities above 3 m/s, the opposite trend is observed. The pressure difference between forward and reverse flow inside the microtexture shows a positive correlation with the lubricant flow rate. Two representative cases with pronounced differences, 1 m/s and 6 m/s, were selected for detailed analysis.

Table 1. Velocity and pressure changes of the Tesla valve microtexture at different flow rates

Lubricating oil flow rate /m • s^{-1}	Forward maximum pressure /kPa	Reverse maximum pressure /kPa	Forward maximum flow rate /m • s^{-1}	Reverse the maximum flow rate /m • s^{-1}

0.5	104.3	109.4	0.791	0.794
1	109.5	111.5	1.423	1.628
2	113.4	139.2	2.945	2.996
3	193.8	141.7	4.585	4.543
6	458.9	272.4	11.361	9.359
9	521.3	321.4	19.203	14.112

Figures 2(a) show the velocity distributions of the lubricant entering the Tesla-valve microtexture in the forward direction at different flow rates. As illustrated, the maximum flow velocity reaches 1.423 m/s at an inlet velocity of 1 m/s and 11.361 m/s at an inlet velocity of 6 m/s. Figures 3(b) present the corresponding streamline plots, revealing that under forward flow most of the fluid travels through the main channel, with only a small fraction entering the curved channel.

Based on Figure 2, the flow-field characteristics of the lubricant entering the Tesla-valve microtexture can be analyzed. As shown in Figure 2(a), when the lubricant enters the channel at 1 m/s, the majority of the fluid flows into Region 1 of the main channel at a relatively high velocity of 1.2 m/s, while only a minor portion branches into Region 2. The pressure drop in Region 2 reduces the velocity to 0.18 m/s, and the overall flow direction inside the microtexture remains relatively uniform. From Figure 2(b), it can be seen that at the channel intersections the fluid impinges on the texture wall and changes direction, producing a velocity gradient. Simultaneously, flow diversion occurs in Region 3, and the impingement of the lubricant on the wall in Region 4 causes a small loss of kinetic energy, reducing the lubricant velocity.

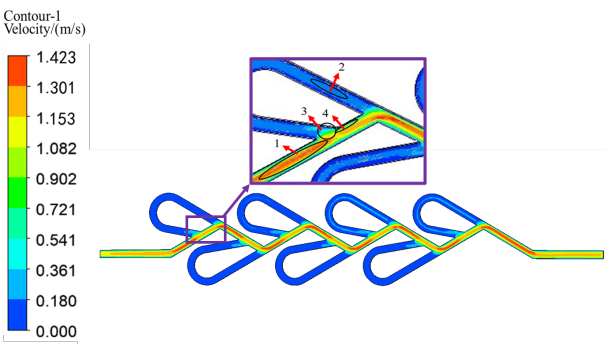

(a) v=1 m/s forward flow velocity diagram

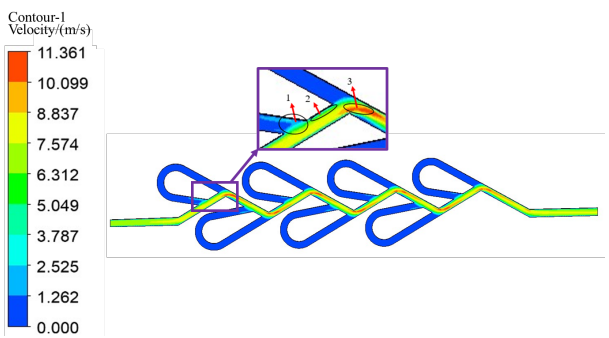

(b) v=6 m/s forward flow velocity diagram

Fig 2. Diagram of forward flow velocity at different initial velocities

By comparing Figures 2 and 3, it can be observed that the lubrication oil flow patterns differ significantly between the reverse and forward velocity fields. As shown in Figure 3(a), during forward flow at 1 m/s, the maximum velocity of the lubricant also occurs in the main channel, reaching 1.628 m/s, while near the outer wall at the bend exit, the velocity decreases to approximately 0.4 m/s. Figure 3(b) illustrates the streamlines of lubricant flowing in reverse at 1 m/s through the Tesla valve, where, after splitting at the bifurcation, the volumetric flow into the curved channel is greater than that in the forward direction. From Figure 3, it is evident that under reverse flow, the velocity distribution of the lubricant is more complex, more turbulent, and exhibits stronger recirculation compared with forward flow. The high-speed jet generated in the straight channel splits at the channel intersection, with part of the fluid entering Region 1. As the fluid passes through the curved channel, its kinetic energy decreases, reaching a minimum at the point of maximum curvature.

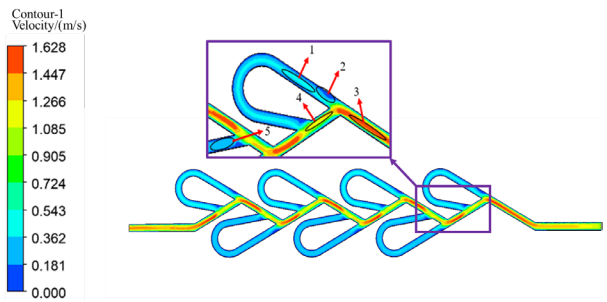

(a) v=1 m/s reverse flow velocity diagram

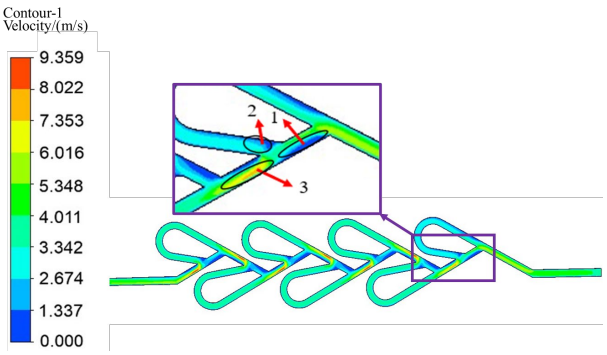

(b) v=6 m/s reverse flow velocity diagram

Fig 3. Reverse flow velocity diagram with different initial velocities

Variations in flow velocity can cause fluctuations in the oil film's load-bearing capacity [10]. By comparing the fluid motion under different flow velocities, it is observed that at a low velocity of 1 m/s, the reverse flow velocity exceeds the forward flow velocity, with a difference of 0.205 m/s. As the flow velocity increases to 6 m/s, the forward flow velocity becomes greater than the reverse flow velocity, and the velocity difference increases to 2.002 m/s. This phenomenon is primarily due to the behavior of the fluid at low velocities: during forward motion, the fluid splits at the channel intersection and partially impacts the channel wall, forming a blockage zone

that reduces the flow velocity. At high forward velocities, the fluid within the bend is sparse, and vortices occur at the intersection, resulting in minimal energy loss due to convective mixing; only the energy loss from fluid-wall impact occurs. This explains why the forward velocity is significantly higher at high flow rates.

Figure 4 presents the total pressure distribution of the lubricant in the Tesla valve microtexture for different flow directions and velocities. Unlike the forward and reverse velocity fields, the pressure fields exhibit certain similarities: the inlet pressure is the highest, and the fluid continuously loses energy during flow. Since the cross-sectional area of the channel does not change, the pressure gradually decreases along the flow direction. As shown in Figures 4(a) and 4(b), at low velocities, the flow velocity does not change significantly, resulting in a relatively uniform pressure distribution in both forward and reverse directions, with only minor pressure disturbances observed at the final bifurcation during reverse flow.

Analysis of Figures 4(c) and 4(d) shows that at higher flow velocities, the pressure distribution of the lubricant differs from that at low velocity. In both forward and reverse flow, pressure disturbances of varying degrees appear at the microtexture intersections. The pressure within the channel increases with the flow velocity of the lubricant, but the increase in forward flow is greater than that in reverse flow. This is because, in Figure 4(c), a larger volumetric flow passes through the main channel during forward flow, and the impact of the fluid on the channel wall converts kinetic energy into pressure potential, which enhances the load-bearing capacity of the oil film and thereby improves lubrication performance. Figure 4(d) indicates that during reverse flow, a larger portion of the lubricant enters the curved channel. Although minimal convective mixing occurs after passing through the bend, the high-speed lubricant impacts the channel walls, generating an impinging force that further enhances the load-bearing effect of the oil film.

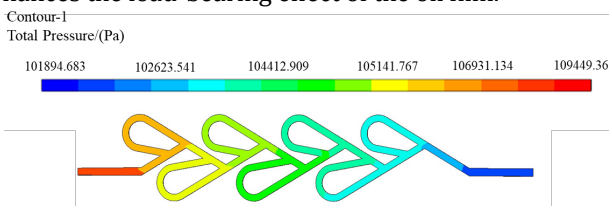

(a) v=1 m/s, total pressure in forward flow

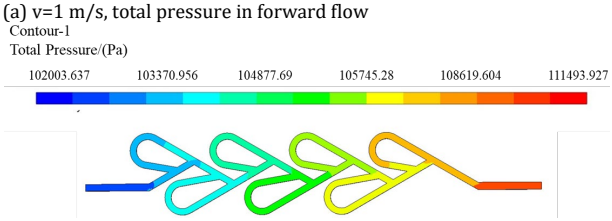

(b) v=1 m/s, total pressure in reverse flow

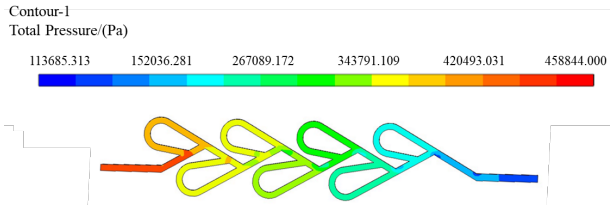

(c) v=6 m/s, total pressure in forward flow

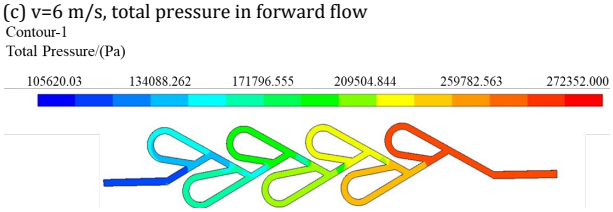

(d) v=6 m/s, total pressure in reverse flow

Fig 4. Contour of the total pressure distribution of the micro-texture of the Tesla valve

3. Conclusion

(1) During fluid motion, phenomena such as convection, impingement, and vortices occur. In forward flow, the load-bearing capacity of the oil film is mainly derived from fluid impingement on the channel walls and vortex effects, whereas in reverse flow, it is dominated by convective effects. Different flow directions have distinct impacts on the oil film load-bearing behavior of the Tesla valve microtexture surfaces.

(2) Under the same experimental conditions, higher pressure corresponds to better oil film load-bearing capacity. At v=1 m/s, the reverse-flow hydrodynamic lubrication performance exceeds that of forward flow, while at v=6 m/s, forward-flow hydrodynamic lubrication performance is higher than reverse flow. Both cases effectively enhance the oil film load-bearing capacity on the material surface, thereby positively contributing to improved lubrication performance.

References

[1] Thomas F, Tomas V, Tomas P. Wear and friction of self-lubricating coatings applied to spur gears in fluid-free aerospace actuation gearboxes[J]. Proceedings of the Institution of Mechanical Engineers, Part J: Journal of Engineering Tribology, 2024, 238(1): 26-43.

[2] Hamilton D B, Walowit J A, Allen C M. A Theory of Lubrication by Micro irregularities[J]. Journal of Basic Engineering, 1966, 88(1):177.

[3] Qian Jinyuan, Chen Minrui, Liu Xueling, et al. A numerical investigation of the flow of nanofluids through a micro Tesla valve[J]. Journal of Zhejiang University-SCIENCE A, 2019, 20(1): 50-60.

[4] Liu Zhe, Shao Wenqi, Sun Yong, et al. Scaling law of the one-direction flow characteristics of symmetric Tesla valve[J]. Engineering Applications of Computational Fluid Mechanics, 2022, 16(1): 441-452.

[5] Huang Feiya, Ren Liancheng, Xie Shuai, et al. Numerical study of flow characteristics and heat transfer mechanism in Tesla valve tube[J]. Results in Engineering, 2024, 21: 101795-.

[6] Duo Jirenqing, Luo Shanming, Chang Xuefeng. Study on hydrodynamic lubrication and friction reduction performance of cylindrical rolls with tesla valve texture[J]. Tribology Transactions, 2023, 66(6): 981-991.

[7] Xie Zongliang, Zhang Hao, Zhao Bin, et al. Effect of turbulence on lubrication behaviors

of a new bearing under bi-misaligned status: Theoretical and experimental study[J]. Mechanical Systems and Signal Processing, 2024, 218: 111547-.

[8] Wang Qingyang, Wu Weifeng, Zhang Ping, et al. Analysis of turbulent cavitation effects on water-lubricated bearing in single screw compressors[J]. Industrial Lubrication and Tribology, 2024, 76(4): 537-544.

[9] Yin Hang, Yang Jiangang, Gu Qianlei. Numerical study on the hydrodynamic lubrication performance improvement of bio-inspired peregrine falcon wing-shaped microtexture[J]. Tribology International, 2024, 191:109049.

[10] Madaparthi A, Penchaliah R, Sankaranarayanan V. Evaluation of tribological performance in contact pairs by implementing the biomimetic surface textures with lubricant flow using CFD techniques[J]. Industrial Lubrication and Tribology, 2024, 76(5): 639-648.